HHS Public Access

Author manuscript

Nanotechnology. Author manuscript; available in PMC 2017 December 27.

Published in final edited form as:

Nanotechnology. 2016 August 05; 27(31): 315103. doi:10.1088/0957-4484/27/31/315103.

A 3D Printed Nano Bone Matrix for Characterization of Breast Cancer Cell and Osteoblast Interactions

Wei Zhu[1], **Nathan J. Castro**[1], **Haitao Cui**[1], **Xuan Zhou**[1], **Benchaa Boualam**[2], **Robert McGrane**[2], **Robert I. Glazer**[3], and **Lijie Grace Zhang**[1,4,*]

[1]Department of Mechanical and Aerospace Engineering, The George Washington University, Washington DC 20052, USA

[2]College of Computer, Mathematical and Natural Sciences, University of Maryland-College Park, College Park, MD 20742, USA

[3]Department of Oncology, and Lombardi Comprehensive Cancer Center, Georgetown University Medical Center, Washington, DC 20007

[4]Department of Biomedical Engineering and Department of Medicine, The George Washington University, Washington DC 20052, USA

Abstract

Bone metastasis is one of the most prevalent complications of late-stage breast cancer, in which the native bone matrix components, including osteoblasts, are intimately involved in tumor progression. The development of a successful *in vitro* model would greatly facilitate understanding the underlying mechanism of breast cancer bone invasion as well as provide a tool for effective discovery of novel therapeutic strategies. In the current study, we fabricated a series of *in vitro* bone matrices composed of a polyethylene glycol hydrogel and nanocrystalline hydroxyapatite of varying concentrations to mimic the native bone microenvironment for the investigation of breast cancer bone metastasis. A stereolithography-based 3D printer was used to fabricate the bone matrices with precisely controlled architecture. The interaction between breast cancer cells and osteoblasts was investigated in the optimized bone matrix. Using a Transwell® system to separate the two cell lines, breast cancer cells inhibited osteoblast proliferation, while osteoblasts stimulated breast cancer cell growth, whereas, both cell lines increased IL-8 secretion. Breast cancer cells co-cultured with osteoblasts within the 3D bone matrix formed multi-cellular spheroids in comparison to 2D monolayers. These findings validate the use of our 3D printed bone matrices as an *in vitro* metastasis model, and highlights their potential for investigating breast cancer bone metastasis.

Keywords

3D printing; nanomaterials; bone model; breast cancer; osteoblast; co-culture

[*]Corresponding Author: Dr. Lijie Grace Zhang, Tel: 202-994-2479, Fax: 202-994-0238, lgzhang@gwu.edu, Address: 800 22nd Street NW Science and Engineering Hall, Room 3590, Washington DC, 20052.

1. Introduction

Late-stage breast cancer commonly invades and metastasizes within the medullary space of long bones. This highly invasive event involves interactions between metastatic tumor cells and the diverse population of normal cells which collectively support the malignancy. Understanding the interplay and cross-talk between breast cancer and the native bone microenvironment are critical for a greater understanding of metastatic cancer progression as well as for developing new and effective treatments. Natural bone undergoes a process of remodeling which involves both osteoclasts, which resorb small masses of bone tissue, as well as new bone formation by differentiating osteoblasts [1]. Cancer metastasis interrupts normal bone remodeling leading to osteolytic metastatic lesions by unregulated osteoclast activity [2]. Despite attempts to target and modulate osteoclast activity to slow lesion progression, inhibition of osteoclasts alone cannot fully halt bone loss and promote bone repair [3]. Equally important is the role that osteoblasts play in the metastatic process. [4]. When breast cancer invades bone, osteoblasts stop synthesizing proteins necessary for bone repair and secrete inflammatory cytokines that stimulate osteoclast activity [5]. In addition, breast cancer cells produce parathyroid hormone-related protein (PTHrP) [6], which stimulates osteoblasts to secrete receptor activator of nuclear factor kB ligand (RANKL) [7]. RANKL in turn enhances osteoclast activity leading to cytolysis and the release of transforming growth factor (TGF-β) from the bone matrix, which results in increased PTHrP. Additionally, several other molecules, such as vascular endothelial growth factor (VEGF) and insulin-like growth factors (IGFs), contribute to this complex process [8, 9].

There are some intrinsic difficulties to study the bone remodeling processes *in vivo* due to the complicated nature of bone and the extensive skeletal system [5], and therefore, it is essential to develop novel in vitro systems that provide a microenvironment to mimic the interactions between breast cancer cells and the native bone microenvironment. Present *in vitro* cancer cell culture models do not recapitulate the pathophysiological features of the tumor microenvironment that lead to cancer progression. Ideally, an *in vitro* model must retain the biological complexity of the native system to assure it is a reasonable surrogate for natural bone. Toward this end, three-dimensional (3D) tissue engineered models have been extensively investigated with the aim of offering *in vitro* systems that provide experimental flexibility while maintaining biological complexity [10] [11]. In 3D models, cells exhibit traits more similar to those expressed *in vivo* in comparison to their two-dimensional (2D) counterparts [12, 13].

Native bone tissue is a nanocomposite composed of a soft hydrogel template and the inorganic mineral nanocrystalline hydroxyapatite (nHA) [14]. For the development of our bone matrices, nHA was incorporated into a polyethylene glycol (PEG)-based hydrogel in order to mimic the structure of natural bone. To accurately control the architecture of our bone model, we employed 3D printing to allow scalability and reproducibility for the layer-by-layer fabrication of pre-designed constructs using computer-aided designed [15]. The well-defined geometry of such 3D cancer cell models makes it possible to directly investigate the relationship of structure to cellular function and gene expression [16]. In the present study, we investigated the interaction between breast cancer cell and osteoblasts on

their proliferation, morphology and cytokine secretion in our novel 3D printed bone matrices.

2. Experimental

2.1 Preparation and characterization of 3D printed bone matrices

Fig. 1 summarizes the fabrication and use of our 3D matrix as well as validation of its efficacy. 3D models with a square pore pattern were designed by computer-aided design (CAD) and printed with a table-top stereolithography-based 3D bioprinter. The printer was developed based on the existing rapid prototyping platform (Printrbot®). It includes a movable stage, a fiber optic-coupled solid-state UV laser, and an X-Y toolhead for motion. Photocross-linked hydrogel solutions were prepared by blending 60 % (w/w) polyethylene glycol-diacrylate (PEG-DA, Mn=700, Sigma-Aldrich), 40 % (w/w) PEG (Mn=300, Sigma-Aldrich) and 0.5 % (w/w) Irgacure 819 as photoinitiator. nHA containing matrices were fabricated by dispersing nHA into the hydrogel solution at concentrations of 2%, 5% and 10% (w/w) of PEG-DA. The synthesis of nHA was detailed in our previous study [17]. A 355 nm ultraviolet (UV) laser was used to crosslink all hydrogel matrices. Matrix was printed as three layers with 400 μm each layer. Matrix morphology was examined by scanning electron microscopy (SEM, Zeiss NVision 40 FIB) after gold coating. In addition, compressive testing was conducted using an electromechanical universal tester equipped with a 100 N load cell (MTS Corporation, US). The cross-head speed was set as 2 mm/min and test was performed under ambient condition.

2.2 Cells culture, adhesion and proliferation study on various matrices

Metastatic breast cancer cell line MDA-MB-231 was obtained from the ATCC and used to evaluate the printed bone matrices. MDA-MB-231 cells were cultured in Dulbecco's-modified Eagle's medium (DMEM, Gibco) supplemented with 10% (v/v) fetal bovine serum and 1% (v/v) penicillin-streptomycin. Human fetal osteoblast cell line hFOB (ATCC) was cultured in a 1:1 mixture of Ham's F12 Medium:Dulbecco's Modified Eagle's Medium (Lonza) containing 2.5 mM L-glutamine and 10% fetal bovine serum. hFOB cell experiments were performed using passages 4–8. All cells were incubated at 37 °C in an atmosphere of 5 % CO_2.

Printed matrices for cell studies were obtained using a 12 mm circular punch. Cell adhesion was performed by seeding MDA-MB 231 cells at a density of 1×10^5 cells/sample and cultured under standard culture conditions for 4 h. Cell number was then assessed by CellTiter 96® AQueous One Solution cell proliferation assay (MTS assay, Promega). Briefly, at predetermined time points, samples were transferred to a fresh well plate. Cells were trypsinized and mixed with MTS, and after 1 h of incubation, absorbance of each sample was measured spectrophotometrically at 490 nm with a scanning multi-well spectrophotometer. For MDA-MB-231 cell proliferation, cells were also seeded at a density of 1×10^5 cells/sample onto the matrices containing varying nHA concentrations, and grown for 1, 3 and 5 days. Cell number was quantified with MTS assay as well.

2.3 Immunofluorescence analysis

MDA-MB-231 cells were cultured at a density of 1×10^5 per matrix for up to 5 days. At day 1, 3 and 5, samples were transferred into a new well-plate after PBS washing, MDA-MB-231 cells were fixed in 10% formaldehyde for 15 min followed by washing in phosphate buffered saline. Cells were then permeabilized with 0.1% Triton X-100 for 5 min at room temperature. The actin cytoskeleton was stained with Texas Red-X phalloidin (Life Technologies) for 40 min, and DNA was stained with DAPI (2-(4-Amidinophenyl)-6-indolecarbamidine dihydrochloride, Sigma-Aldrich) for 10 min, and visualized using a laser scanning confocal microscope (ZEISS LSM 710).

2.4 Indirect co-culture of MDA-MB-231 and hFOB cells

In order to investigate the interaction between MDA-MB-231 and hFOB cells proliferation, we utilized a 12-well Transwell® co-culture system. Circular printed matrices measuring 12 mm and 22 mm in diameter (all samples perfectly fit the upper and lower wells), were placed in the upper chamber (12 mm in diameter, 0.4 μm pore size, Sigma-Aldrich) and lower well, respectively. Due to the fragility of the membrane in the upper chamber, we quantified cell number in the lower chamber for four groups. Specifically, to measure the influence of co-culture on MDA-MB-231 cell proliferation, hFOB cells were seeded on the printed bone matrices in the upper well, and MDA-MB-231 cells were seeded on the matrix in the lower well (Fig. 5A, group 1). Cell culture of MDA-MB-231 alone was selected as control (Fig. 5A, group 2), and MDA-MB-231 cell number was determined in both lower chambers (group 1 and 2) after removing the upper well. Similarly, hFOB cell number was measured in the lower wells (Fig. 5B, groups 3 and 4). MDA-MB-231 and/or hFOB cells were seeded in the upper and lower wells at a density of 1×10^5 per sample. After 1, 3 and 5 days culture, cell number was quantified by the MTS assay.

2.5 Cytokine analysis

Cytokine secretion from MDA-MB-231 and hFOB cells in the Transwell® system was analyzed using conditioned medium. MDA-MB-231 and hFOB cells were co-cultured in the Transwell® system for 24 h at a cell density of 5×10^5 per matrix. hFOB cells were seeded on the matrix in the lower well, and MDA-MB-231 cells were seeded on the matrix in the upper well. After 24 h, the Transwell was removed and hFOB cells in the lower well were transferred to fresh plates. After rinsing with PBS, hFOB cells were incubated in serum-free DMEM/F12 medium for another 24 h. For similar experiments using MDA-MB-231 cells, serum-free DMEM medium was used. Conditioned media was then collected, centrifuged to remove cellular debris, and IL-8 was quantified using a human IL-8 ELISA Kit (Boster Biological Technology) per the manufacturer's instructions. Total protein was measured using a protein assay kit (Thermo-Scientific) and IL-8 levels were normalized to total protein.

2.6 Co-culture of MDA-MB-231 and hFOB cells

To study the effects of osteoblasts on breast cancer cell morphology, hFOB and MDA-MB-231 cells were directly co-cultured on the bone matrix. Prior to seeding, MDA-MB-231 and hFOB cells were pre-labeled with CellTracker Orange (Life Technologies) and

CellTracker Green (Life Technologies), respectively, per the manufacturer's instruction, and 5×10^5 hFOB and 5×10^5 MDA-MB-231 cells were co-cultured for 7 days. On days 1, 3, 5 and 7, cells were fixed with 10 % formaldehyde for 15 min and imaged by confocal microscopy.

2.7 Statistical analysis

Statistical analysis was carried out using one-way ANOVA and Student's t-test. For quantitative experiments, data are presented as mean ± standard deviation; sample size is greater than or equal to 5. Statistical significance was defined as $p<0.05$ in all analyses.

3. Results

3.1 Porous structure of printed bone matrices

Stereolithography-based 3D printing permits the fabrication of porous constructs with well-defined architecture and integrated nanomaterials. SEM micrographs (Fig. 2) show that the addition of nHA did not affect printing resolution as illustrated by the similar pore size amongst the various matrices. All printed matrices had a clearly defined square pattern and nHA was well dispersed within the entire matrix at all concentrations. Stiffness of printed matrices increased as a function of nHA concentration. A 127% increase in compressive modulus was found in 10% nHA containing matrix when compared to the matrix without nHA.

3.2 Improved MDA-MB-231 cell growth on nHA-containing matrices

The adhesion and proliferation of MDA-MB-231 cells on the matrices with varying nHA concentration was next determined (Fig. 3). There is no significant difference on 4 h adhesion amongst the 3D printed matrices with increasing nHA concentration (Fig 3A). When compared to matrices containing PEG-DA hydrogel alone, cellular proliferation after 3 days was significantly higher on matrices containing nHA, especially at 10% nHA. After 5 days, cell proliferation on 2%, 5% and 10% nHA-containing matrices was increased by 63%, 69% and 87%, respectively vs. PEG-DA alone (Fig 3B).

To further evaluate the effectiveness of our matrix, confocal microscopy was used to assess cell spreading, proliferation and actin development on matrices as a function of nHA concentration (Fig. 4). After one day in culture, MDA-MB-231 attached upon the 3D printed matrices displaying good actin expression. An evident increase in cell number with time was observed amongst all groups. These findings indicate that the nHA-containing PEG-based hydrogel matrix provides a biocompatible and supportive microenvironment for breast cancer cell attachment and proliferation.

3.3 Crosstalk between MDA-MB-231 and hFOB cells

Using the Transwell cell culture system, MDA-MB-231 cells were cultured on the 10% nHA matrix in the lower well and hFOB cells in the upper well to allow for the exchange of medium and secreted cytokines while physically separating the two cell lines. As a control, MDA-MB-231 cells were grown in the absence of hFOB cells. MDA-MB-231 cells grown in the presence of hFOB cells exhibited a significant increase in proliferation after 3 and 5

days (Fig. 5A). When the converse was tested, MDA-MBA-231 cells reduced the proliferation of hFOB cells (Fig. 5B).

3.4. Crosstalk between MDA-MB-231 and hFOB cells increases cytokine secretion

To investigate osteoblast cell function, IL-8 was analyzed in the Transwell system and in monolayer cultures. After 24 h, hFOB cells produced a 3-fold greater amount of IL-8 in the presence of MDA-MB-231 cells in comparison to hFOB monolayers (Fig. 6A). Similarly, IL-8 production from MDA-MB-231 also increased when grown in the presence of hFOB cells (Fig. 6B).

3.5. Cellular organization in a 3D matrix vs. monolayer culture

2D cell culture-based tumor models have been used extensively in preclinical drug discovery for several decades [18], although they serve as poor predictive models of clinical success. In contrast, the use of 3D cancer cell spheroid cultures may be more representative of tumor-initiating cells and serve as a more effective tool for drug screening [13]. Multicellular spheroids closely resemble the natural tumor structure *in vivo*. Therefore, several approaches have been explored to obtain a suitable tumor spheroid model. With this in mind, MDA-MB-231 and hFOB cells were co-cultured on the matrix to measure their capacity for spheroid formation. Notably, cells grown on printed matrices were morphologically spherical and actively aggregated even at early culture time points (Fig. 7). Cells grown on 2D surface, by contrast, formed flat monolayered structures without any spherical morphology after 7 days. In the 2D culture system, MDA-MB-231 cells exhibited apparent inhibition of hFOB cell growth and development. MDA-MB-231 cells were dominant (red signal in Fig. 7) in the monolayer culture at day 5 as illustrated by confocal microscopy. There was almost no hFOB cells evident after 7 days. This phenomenon is partially ascribed to a faster rate of proliferation for MDA-MB-231 cells. On the other hand, the cytokines secreted from MDA-MB-231 cells also contributed to the limited growth of hFOB cells. In the printed bone matrix, two types of cells formed small and compact spheroids with a diameter of ~100 μm at day 7. Additionally, the matrix showed less cellular inhibition to hFOB cells after 7 days co-culture.

4. Discussion

Animal and monolayer cell culture models have been extensively used over the last two decades to study cancer cell growth and to identify new anticancer agents [19]. Animal models provide a physiological environment resembling human conditions, but they are expensive, labor intensive and when used for human tumor xenografts, lack an intact immune system. Monolayer cultures also have limitations, including lack of spheroidal morphology and aberrant integrin signaling [20, 21]. In contrast, 3D culture systems composed of more than one cell type permit a more biomimetic microenvironment [22, 23]. In this study, we developed an artificial bone matrix using stereolithography-based 3D printing, which generated a biomimetic environment sufficient for studying the interaction between breast cancer cells and osteoblasts.

The matrix contained nHA, the calcium phosphate found in mature bones, which plays an active role in amplifying the progression of breast cancer metastases to bone [24, 25]. Addition of nHA to the bone matrix increased the proliferation rate of breast cancer cells in a concentration-dependent manner, which was attributed in part to the mitogenic effect of nHA [26]. Pathi et al found that nHA can modulate protein adsorption which may directly contribute to improved cell proliferation [24]. Adsorbed RGD-containing proteins may be involved in this effect as these proteins have been shown to regulate proliferative signaling pathway [27]. Additionally, the upregulation of matrix metalloproteinases by nHA, such as MMP-2, -9, and -13, in breast cancer cells, may have contributed to this effect [26]. Therefore, nHA was incorporated into the matrix to maximize mimicking the physiological complexity of native bone.

Human breast cancer cells co-cultured with hFOB cells on the matrix directly affected the morphology, proliferation rate, and cytokine secretion of osteoblasts. IL-8 secretion by osteoblasts was enhanced in the presence of MDA-MB-231 cells. IL-8 (Cxcl8) is a multifunctional pro-inflammatory chemokine that inhibits bone alkaline phosphatase expression, decreases normal bone resorption, and increases osteoclast motility at new resorption sites [28, 29]. IL-8 is highly expressed in breast cancer and contributes to angiogenesis and invasion during tumorigenesis [30]. Kinder et al. found that conditioned media from metastatic breast cancer cells could induce osteoblast cells to express increased levels of IL-8 [31]. Similar osteoblast behavior was seen in our 3D matrix system (Fig. 6), where in addition, we found that osteoblasts stimulated breast cancer cell IL-8 secretion. As reported by Fong et al., osteoblast conditioned medium is able to activate an IL-8 promoter in human breast cancer resulting in increased IL-8 transcription and protein synthesis [32]. Therefore, our matrix provides a biomimetic microenvironment for both osteoblasts and breast cancer cells that allows them to interact physiologically.

Cancer invasion to bone is associated with osteoblast recruitment, which in turn enhances tumor growth [33]. Traditional monolayer cell culture fails to mimic the multicellular spheroid structure due to the strong physical contact between cells and 2D substrate [21]. In contrast, the addition of a third culture dimension promotes cellular spheroid formation, which is considered to have increased tumor-initiating potential [34]. Since tumors are composed of many cell populations, the formation of multicellular spheroids in the matrix may more closely approximate the tumor microenvironment [35].

5. Conclusions

Stereolithography-based 3D printing is capable of fabricating artificial bone matrices using natural bone nanomaterial with well-defined architecture. The matrix was capable of hosting breast cancer cells and osteoblasts and stimulating cell proliferation and cytokine secretion as multi-cellular spheroids. Therefore, these matrices should be useful for examining biological processes associated with bone metastasis.

Acknowledgments

The authors would like to thank GW Katzen Cancer Research Center Innovative Cancer Pilot Research Grant and NIH Director’s New Innovator Award 1DP2EB020549-01 for financial support.

References

1. Sims NA, Martin TJ. Coupling the activities of bone formation and resorption: a multitude of signals within the basic multicellular unit. BoneKEy reports. 2014; 3:481. [PubMed: 24466412]
2. Chen YC, Sosnoski DM, Mastro AM. Breast cancer metastasis to the bone: Mechanisms of bone loss. Breast Cancer Research. 2010; 12(6):215–215. [PubMed: 21176175]
3. Mastro AM, et al. Breast cancer cells induce osteoblast apoptosis: A possible contributor to bone degradation. Journal of Cellular Biochemistry. 2004; 91(2):265–276. [PubMed: 14743387]
4. Hsu YL, et al. Breast tumor-associated osteoblast-derived CXCL5 increases cancer progression by ERK/MSK1/Elk-1/Snail signaling pathway. Oncogene. 2013; 32(37):4436–4447. [PubMed: 23045282]
5. Krishnan V, Vogler EA, Mastro AM. Three - Dimensional in Vitro Model to Study Osteobiology and Osteopathology. Journal of Cellular Biochemistry. 2015; 116(12):2715–2723. [PubMed: 26039562]
6. Guise TA. Molecular mechanisms of osteolytic bone metastases. Cancer. 2000; 88(12 Suppl):2892–2898. [PubMed: 10898330]
7. Yin JJ, Pollock CB, Kelly K. Mechanisms of cancer metastasis to the bone. Cell Res. 2005; 15(1): 57–62. [PubMed: 15686629]
8. Bendre MS, et al. Expression of interleukin 8 and not parathyroid hormone-related protein by human breast cancer cells correlates with bone metastasis in vivo. Cancer Research. 2002; 62(19): 5571–5579. [PubMed: 12359770]
9. Guise TA, Yin JJ, Mohammad KS. Role of endothelin - 1 in osteoblastic bone metastases. Cancer. 2003; 97(S3):779–784. [PubMed: 12548575]
10. Xu X, Farach-Carson MC, Jia XQ. Three-dimensional in vitro tumor models for cancer research and drug evaluation. BIOTECHNOLOGY ADVANCES. 2014; 32(7):1256–1268. [PubMed: 25116894]
11. Nelson CM, Bissell MJ. Modeling dynamic reciprocity: Engineering three-dimensional culture models of breast architecture, function, and neoplastic transformation. Seminars in Cancer Biology. 2005; 15(5):342–352. [PubMed: 15963732]
12. Birgersdotter A, Sandberg R, Ernberg I. Gene expression perturbation in vitro—A growing case for three-dimensional (3D) culture systems. Seminars in Cancer Biology. 2005; 15(5):405–412. [PubMed: 16055341]
13. Charoen KM, et al. Embedded multicellular spheroids as a biomimetic 3D cancer model for evaluating drug and drug-device combinations. BIOMATERIALS. 2014; 35(7):2264–2271. [PubMed: 24360576]
14. Zhang L, Webster TJ. Nanotechnology and nanomaterials: Promises for improved tissue regeneration. Nano Today. 2009; 4(1):66–80.
15. Holmes B, et al. Development of Novel Three-Dimensional Printed Scaffolds for Osteochondral Regeneration. TISSUE ENGINEERING PART A. 2015; 21(1–2):403–415. [PubMed: 25088966]
16. Hamilton G. Multicellular spheroids as an in vitro tumor model. Cancer Letters. 1998; 131(1):29–34. [PubMed: 9839617]
17. Wang M, et al. Design of Biomimetic and Bioactive Cold Plasma-Modified Nanostructured Scaffolds for Enhanced Osteogenic Differentiation of Bone Marrow-Derived Mesenchymal Stem Cells. TISSUE ENGINEERING PART A. 2014; 20(5–6):16–1071.
18. LaBarbera DV, Reid BG, Yoo BH. The multicellular tumor spheroid model for high-throughput cancer drug discovery. Expert Opinion on Drug Discovery. 2012; 7(9):819–830. [PubMed: 22788761]
19. Yamada KM, Cukierman E. Modeling Tissue Morphogenesis and Cancer in 3D. Cell. 2007; 130(4):601–610. [PubMed: 17719539]
20. Mizushima H, et al. Integrin signal masks growth-promotion activity of HB-EGF in monolayer cell cultures. Journal of Cell Science. 2009; 122(23):4277–4286. [PubMed: 19887590]

21. Yoshii H, et al. The use of nanoimprinted scaffolds as 3D culture models to facilitate spontaneous tumor cell migration and well-regulated spheroid formation. Biomaterials. 2011; 32(26):6052–6058. [PubMed: 21640378]
22. Ghajar CM, Bissell MJ. Tumor engineering: The other face of tissue engineering. Tissue Engineering - Part A. 2010; 16(7):2153–2156. [PubMed: 20214448]
23. Zhu W, et al. Engineering a biomimetic three-dimensional nanostructured bone model for breast cancer bone metastasis study. ACTA BIOMATERIALIA. 2015; 14:164–174. [PubMed: 25528534]
24. Pathi SP, et al. Hydroxyapatite nanoparticle-containing scaffolds for the study of breast cancer bone metastasis. Biomaterials. 2011; 32(22):5112–5122. [PubMed: 21507478]
25. Zhu W, et al. 3D printed nanocomposite matrix for the study of breast cancer bone metastasis. Nanomedicine: Nanotechnology, Biology and Medicine. 2016; 12(1):69–79.
26. Morgan MP, et al. Calcium hydroxyapatite promotes mitogenesis and matrix metalloproteinase expression in human breast cancer cell lines. Molecular Carcinogenesis. 2001; 32(3):111–117. [PubMed: 11746823]
27. García AJ, Vega MD, Boettiger D. Modulation of cell proliferation and differentiation through substrate- dependent changes in fibronectin conformation. Molecular Biology of the Cell. 1999; 10(3):785–798. [PubMed: 10069818]
28. Bendre MS, et al. Interleukin-8 stimulation of osteoclastogenesis and bone resorption is a mechanism for the increased osteolysis of metastatic bone disease. Bone. 2003; 33(1):28–37. [PubMed: 12919697]
29. Fuller K, Owens JM, Chambers TJ. Macrophage inflammatory protein-1 alpha and IL-8 stimulate the motility but suppress the resorption of isolated rat osteoclasts. The Journal of Immunology. 1995; 154(11):6065–6072. [PubMed: 7751648]
30. Hartman ZC, et al. Growth of triple-negative breast cancer cells relies upon coordinate autocrine expression of the proinflammatory cytokines IL-6 and IL-8. Cancer Research. 2013; 73(11):3470–3480. [PubMed: 23633491]
31. Kinder M, et al. Metastatic breast cancer induces an osteoblast inflammatory response. Experimental Cell Research. 2008; 314(1):173–183. [PubMed: 17976581]
32. Fong YC, et al. Osteoblast-derived TGF-beta 1 stimulates IL-8 release through AP-1 and NF-kappa B in human cancer cells. JOURNAL OF BONE AND MINERAL RESEARCH. 2008; 23(6):961–970. [PubMed: 18435575]
33. Guise TA, Weilbaecher KN, McCauley LK. Cancer to bone: a fatal attraction. Nature Reviews Cancer. 2011; 11(6):411–425. [PubMed: 21593787]
34. Al-Hajj M, et al. Prospective Identification of Tumorigenic Breast Cancer Cells. Proceedings of the National Academy of Sciences of the United States of America. 2003; 100(7):3983–3988. [PubMed: 12629218]
35. Alessandri K, et al. Cellular capsules as a tool for multicellular spheroid production and for investigating the mechanics of tumor progression in vitro. Proceedings of the National Academy of Sciences. 2013; 110(37):14843–14848.

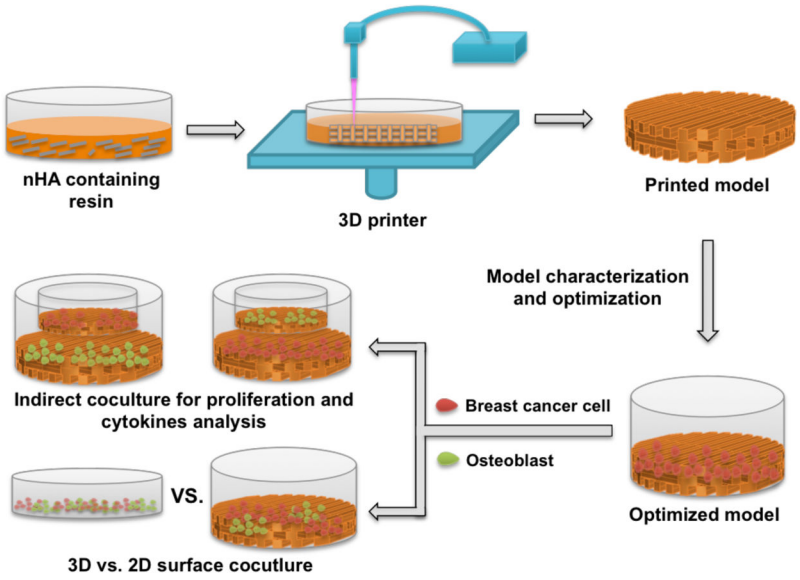

Figure 1.
A schematic illustration of 3D printed bone matrix fabrication and validation.

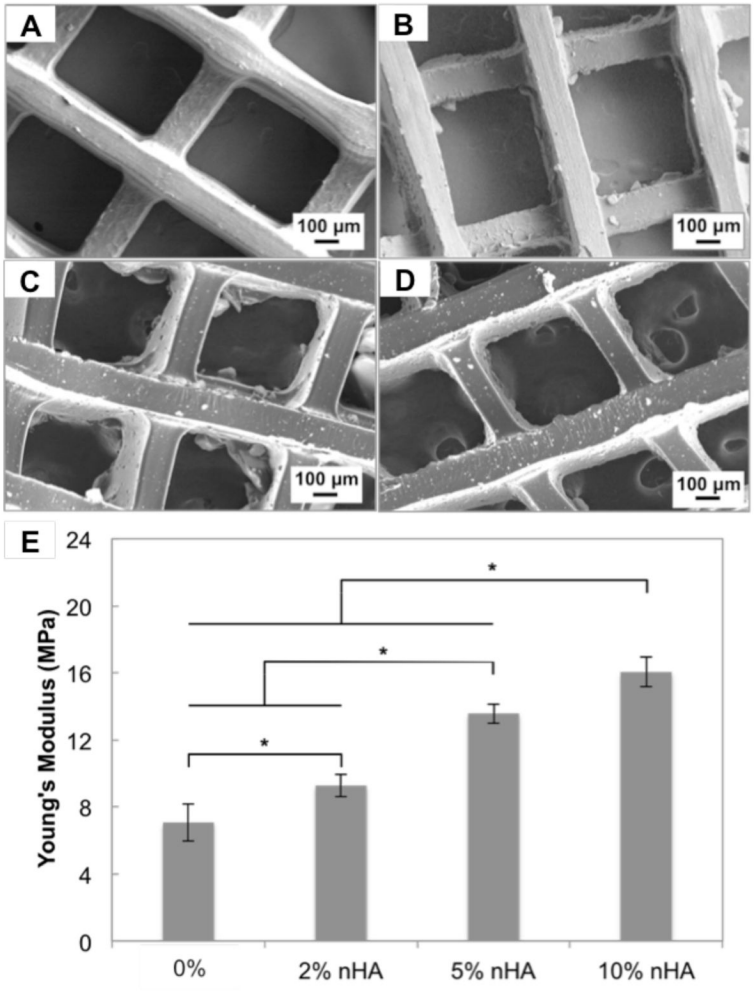

Figure 2.

SEM images of printed bone matrices. A, Control without nHA or with B, 2 % nHA, C, 5 % nHA and D, 10 % nHA. (E) Young's modulus of various matrices. Data are presented as mean ± standard deviation; n=3; *p<0.05.

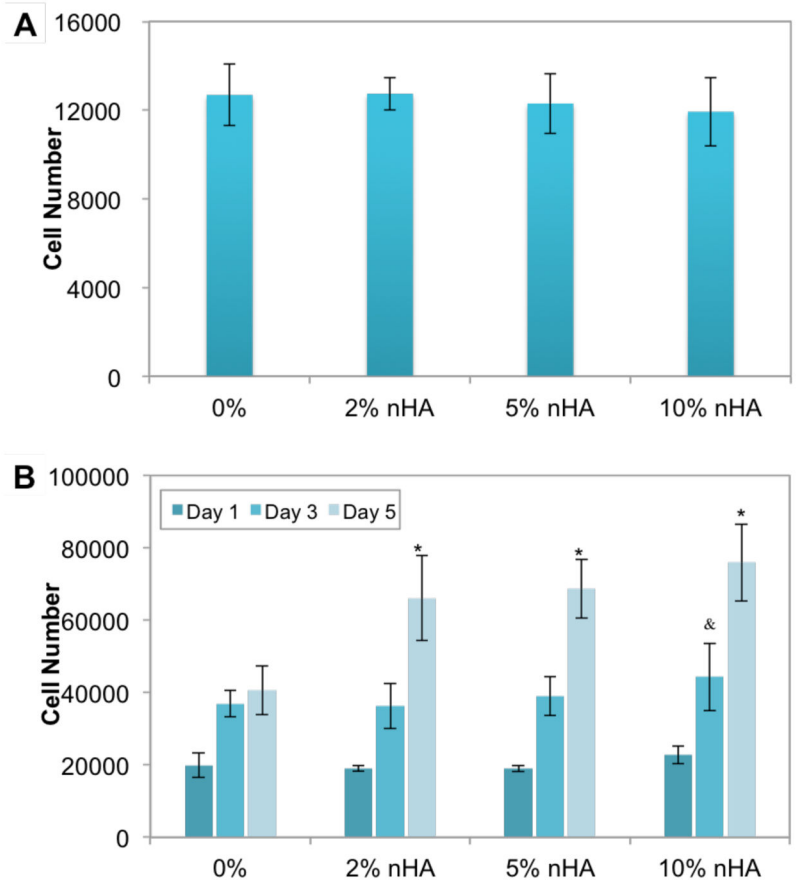

Figure 3.

The (A) adhesion and (B) proliferation of MDA-MB-231 cells on matrices of varying nHA concentration. Data are presented as mean ± standard deviation; N=9; &, $p<0.05$ vs. control at day 3; *, $p<0.05$ vs. control at day 5.

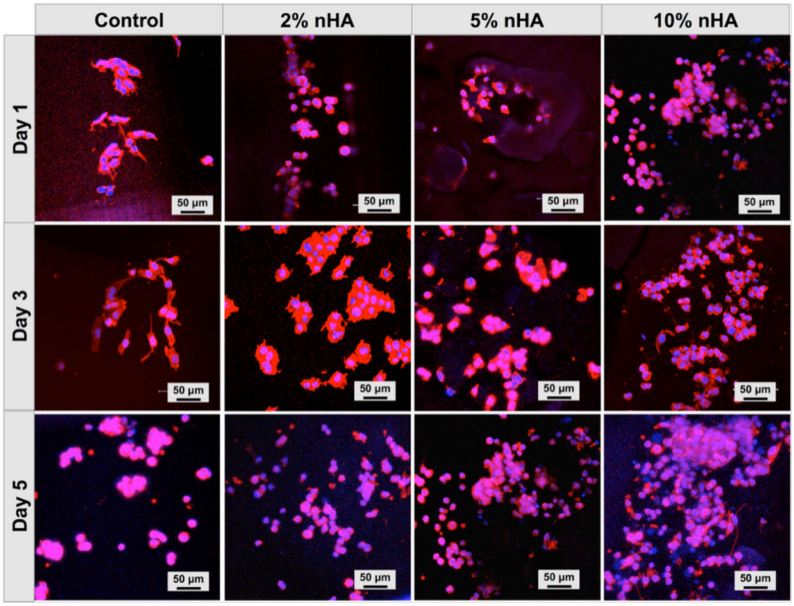

Figure 4.

Confocal microscopy of MDA-MB-231 cells on matrices with varying nHA concentrations after incubation for 1, 3, and 5 days. Cells were stained for actin using Texas Red-X phalloidin (red) and for DNA using DAPI (blue).

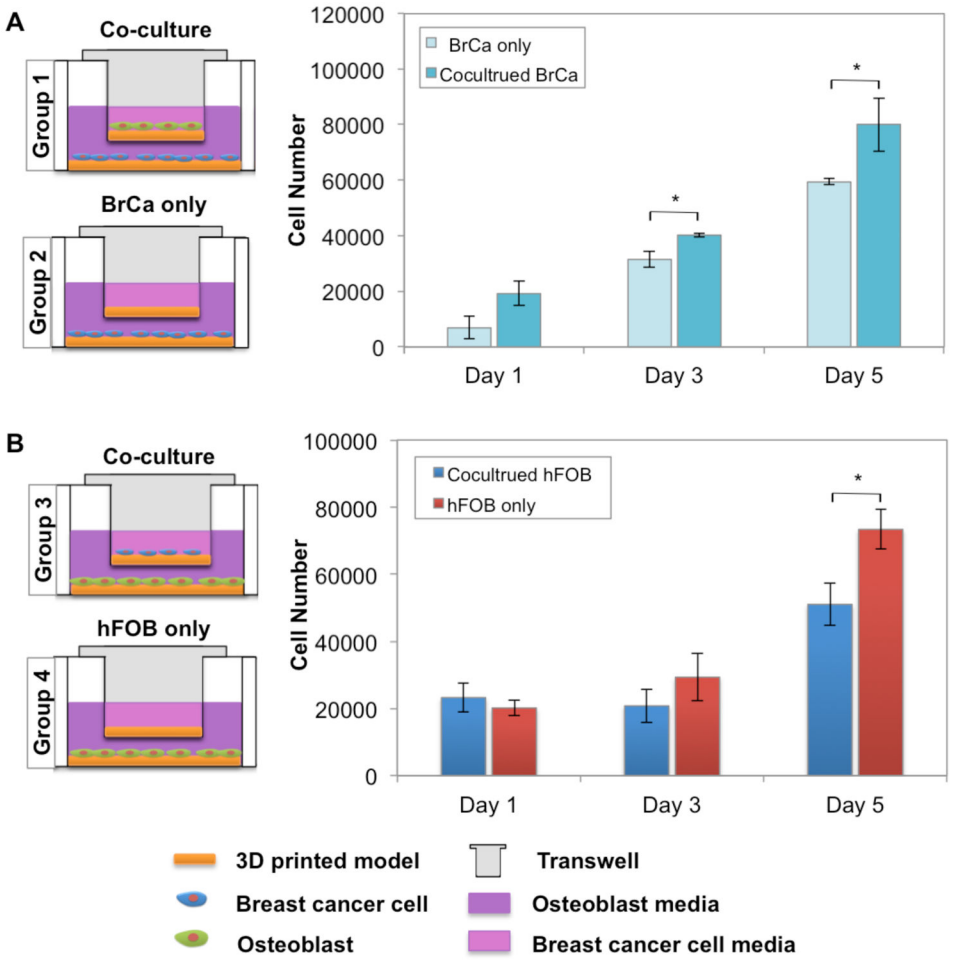

Figure 5.

The influence of co-cultured MDA-MB-231 and hFOB cells on proliferation. Illustration of the Transwell® culture system. Co-culture of MDA-MB-231 and hFOB cells (A) enhanced MDA-MB-231 proliferation, whereas, hFOB cell proliferation was reduced (B) in comparison to monolayer culture. Data are presented as mean ± standard deviation; N=9; *, $p<0.05$. All cell proliferation data were collected from the cells on the bottom chamber.

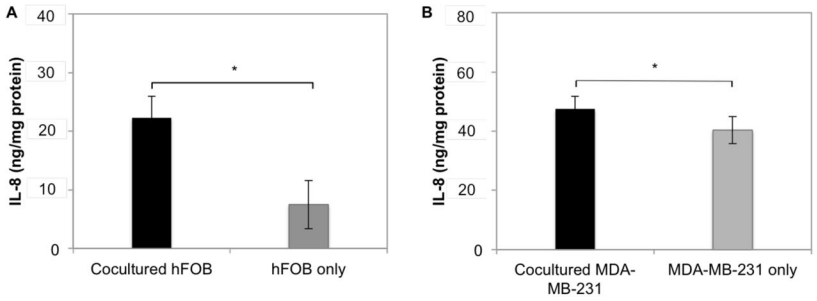

Figure 6.

Increased IL-8 production by hFOB (A) and MDA-MB-231 (B) in the Transwell culture system. Data are presented as mean ± standard deviation; N=5; *, $p<0.05$.

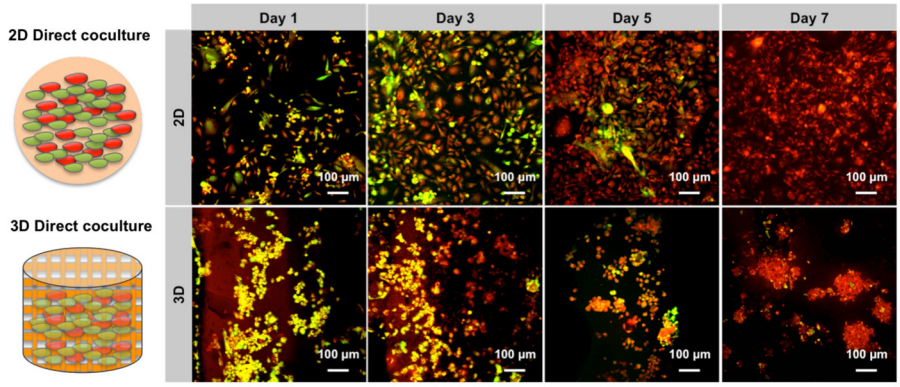

Figure 7.

Enhanced spheroid formation by direct co-culture of hFOB and MDA-MB-231 cells on the 3D matrix in comparison to monolayer culture. hFOB and MDA-MB-231 were pre-stained with cell tracker green and red, respectively, prior to cell seeding.